Intelligent Manufacturing Principles for Structural Health Monitoring in Advance Composite Structures: A Machine Learning-Based Driven Placement Approach

SEAN PSULKOWSKI, BRYANT RODRIGUEZ,
ABDULLAH NOMAN, SERGIO TORINO and TARIK DICKENS

ABSTRACT

This paper presents a fundamental investigation into the composition and placement of mechanoluminescence smart material ink to develop a predictive model framework for machine learning-based lead placement in structural health monitoring of next-generation fabrication methods. To address the need for multifunctionality and structural health monitoring capabilities in next-generation composite structures, this study proposes a closed-loop integration of material-driven design, multi-modal additive processing, and intelligent manufacturing principles. The proposed method utilizes mechanical simulations and in-situ sensing to establish a priori knowledge to optimize the placement, orientation, and manufacturing conditions for smart sensor embedment to maximize sensing efficiency and part performance. Experimental validation involved the hybrid machining of compact tension samples to produce a crack front in additively manufactured material. Microfluidic deposition facilitated mechanoluminescent sensor embodiment near the crack front, and the sample was then subjected to a fracture mechanic analysis, whereby the crack growth rate and direction was monitored. The resulting light emission from the sensor was captured using a mixture of high-speed video and optical sensors to determine the mechanical energy transferred during crack propagation. The resulting dataset informed an algorithmic approach to govern the placement and process parameters of the embedded mechanoluminescent sensors throughout the polymeric structure. This approach enriches the knowledge pool of digital design discovery, showcasing the capabilities of material-driven learning schema for multifunctional composite fabrication. Our investigation provides important insights into the design and development of next-generation materials with enhanced structural health monitoring capabilities. This approach provides a valuable tool for the real-time monitoring of crack propagation and material failure, which has important implications for the development of safe and reliable structures in various industrial applications.

INTRODUCTION

Embedding sensors in composite materials has proven to be difficult when creating

Sean Psulkowski, PhD Candidate, Email: scp13e@fsu.edu. High Performance Materials Institute (HPMI), Department of Industrial and Manufacturing Engineering, Florida State University, Tallahassee, FL, USA.

intelligent structures and self-sensing motifs. Conducting such precise and benign operations is critical for fabricating sound structural units with multifunctional performance needed to achieve the industry's third generation composites. The concept of mechanoluminescence (ML) has been present since the early 19th century, although the majority of experimental work and applications arrived in recent years, advances in materials science and engineering techniques, have made the incorporation of this phenomenon a feasible alternative failure-stress detection [1]. Furthermore, this leads to the development of new materials with improved properties; and by shedding light on the underlying processes that occur within the deformation of materials at the micro- and nanoscale, ML has the potential to revolutionize the direction to design, create, and test new materials for a wide range of applications in various fields. (e.g., aerospace, biomedical engineering, etc.).

ML, or the phenomenon of light emission from materials upon mechanical deformation, holds great promise for exploring various materials and their failure properties as a contactless sensor. However, the largest limitation for widescale use is its susceptibility to interference: as environmental factors such obstructions, other sources of light, or unexpected failure modes can interfere with the detection or emission of ML all together. To overcome these limitations, various approaches would be performed; based on those practices, recent ML incorporations have exhibited prominent outcomes. An effective and reliable mechanism could be the utilization of ultra-sensitive capturing techniques such as high-speed cameras [2] or photomultipliers [3], but the material driven integration of ML sensors in composite structures has been limited.

This paper presents a fundamental investigation into the composition and placement of ML smart material ink to develop an algorithmic framework for machine learning-based lead placement in structural health monitoring of next-generation fabrication methods. Thus, this article addresses the need for multifunctionality and structural health monitoring capabilities in next-generation composite structures, this study proposes a closed-loop integration of material-driven design, multi-modal additive processing, and intelligent manufacturing principles by producing smart composite structures for sensing and visualization. By implementing these advanced technologies, we can enhance the sensitivity and accuracy of ML-based sensing, enabling its widescale use in diverse applications.

METHODOLOGY

MATERIAL SELECTION

Zinc sulfide (ZnS) is a common inorganic crystal that is known to exhibit ML properties when doped with small amounts of manganese (Mn). This highly efficient ML material (i.e. ZnS:Mn, Phosphor Technology, U.K.) that has a high sensitivity to mechanical stress and a relatively long decay time of its ML emission, was chosen as a material of study. When subjected to mechanical deformation, the ZnS:Mn crystal changes the crystal lattice which causes the electrons in the material to become excited and jump to higher energy levels. These excited electrons then emit light as they relax back to their ground state, resulting in the observed ML [4].

COMPACT TENSION SAMPLE FABRICATION

The fabrication of the compact tension (CT) samples involved a multi-step process, combining the additive manufacturing of with Black Polymaker PolyMax PLA filament and inline direct ink writing of Dymax 9663 UV curable resin formulated to act as an ML-resin solution. This hybrid manufacturing approach allowed for the precise embedding of ML material within predefined cavities, enabling the creation of structural health monitoring samples in custom geometries to deliberately alter crack growth. This experimental fabrication method offered a means to optimize both the shape and placement of the ML material for enhanced ML response under mechanical loading.

The fabrication criteria for material extrusion entailed a 0.4 mm nozzle at 0.2 mm layer height, deposited at 220 C with 100% rectilinear infill. Whereas the direct ink writing required a 1mm nozzle and 140Psi to extrude the ML resin solution; formulated by centrifugally mixing 30 weight percent of ZS:Mn powder averaging 28.2 ± 26 um in diameter. The material properties relevant to the stock material utilized are listed in Table I.

TABLE I. Material Properties

Material	Elastic Modulus (MPA)	Tesnile Strength (MPA)
PLA Filament	2340	63
Neat Resin	668	36

The entire process was carried out using an nScrypt n300 printer, which extruded PLA filament layer by layer to build the CT sample structure, in which the samples were subjected immediately to inline direct ink writing to deposit the ML resin solution into predefined cavities within the printed structure. Once the predefined volume was filled, a UV cure of 337.5 mW/cm2 was performed at a working distance of 6 mm for 180 s. The inline process allowed for accurate placement of the ML material, ensuring optimal distribution and contact with potential stress concentration areas, and a near-instant cure to preserve the homogeneity of the deposited solution.

MECHANICAL TESTING

Compact tension (CT) is widely used to study the fracture behavior of materials, by measuring the crack growth rate, critical crack size, and the load-displacement curve. These parameters provide information about the material's resistance to crack growth and failure, which can be used to evaluate the material's performance under different loading conditions, given a pre-prescribed notch geometry as indicated in Figure 1B.

Tests were carried out under a modified testing regime for polymer-based materials under ASTM E647. Our experimental setup involved the use of the MTS Insight 1-Electromechanical Testing machine, equipped with a 1kN capacity load cell. To ensure the specimen could be broken, the thickness was modified to 3mm. Data acquisition at a rate of 50 Hz and a test speed or strain rate of 100 mm/min was maintained. Additionally, an in-house apparatus was machined to carry out CT testing to allow for imagery of the luminescent events shown in Figure 1A. This modification allowed one full side of the

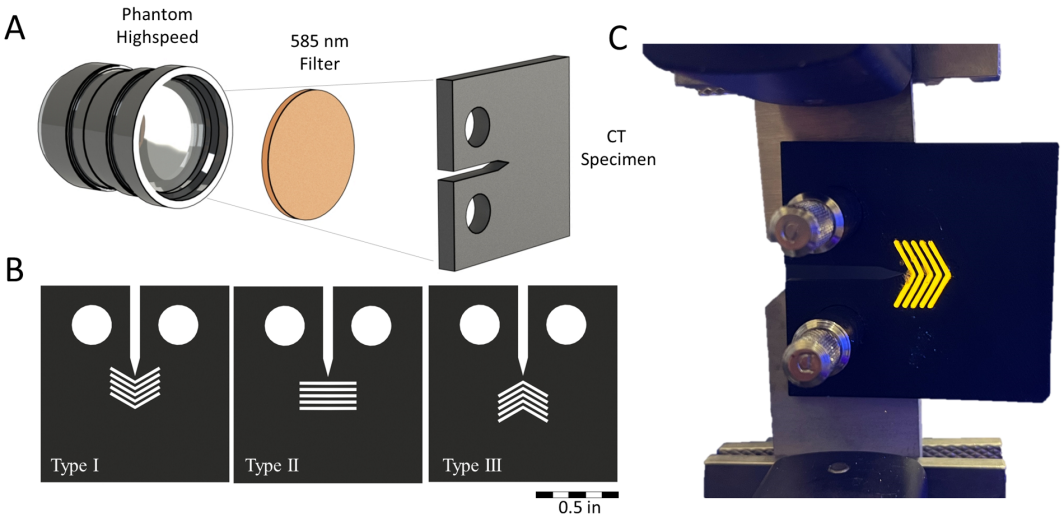

Figure 1. Illustration of the data acquisition system with filtering at 585 nm of a compact tension specimen (a). Sample geometry used in investigation (b) The real image of the printed and fabricated multifunctional tension samples under compact tension load using a modified mechanical apparatus under the 1kn MTS Insight. A blacklight illuminates the geometry of the embedded sensors (c).

multifunctional composite CT samples and apparatus to be in view.

HIGH-SPEED IMAGE CAPTURE

To qualify light emittance during testing, imaging was performed using a V210 Phantom camera (Vision Research) utilized to capture the mechanical testing and failure propagation of the in operando notched specimen. The V210 is a CMOS-style camera with 1280 x 800 sensor, with sensitivity from an active pixel size of 20 microns. The system can achieve approximately greater than $2,000$ frames per second at full resolution. To assist in event detection and luminescent imaging, a 585 nm filter was utilized to screen out ambient light as seen in Figure 1C.

RESULTS AND DISCUSSIONS

MECHANO-VISUALIZATION

Due to its high sensitivity to mechanical stress and long decay time of ML emission, ZnS:Mn can be used for the study of time-resolved phenomena, making it a powerful tool for investigating the behavior of materials under different loading conditions. Figure 2 presents a time-lapse sequence capturing the phenomenon of light emission as a crack propagates through the ML-resin sensors embedded within the sample under loading. This visual depiction offers insights into the intricate interplay between mechanical deformation and the accompanying ML response.

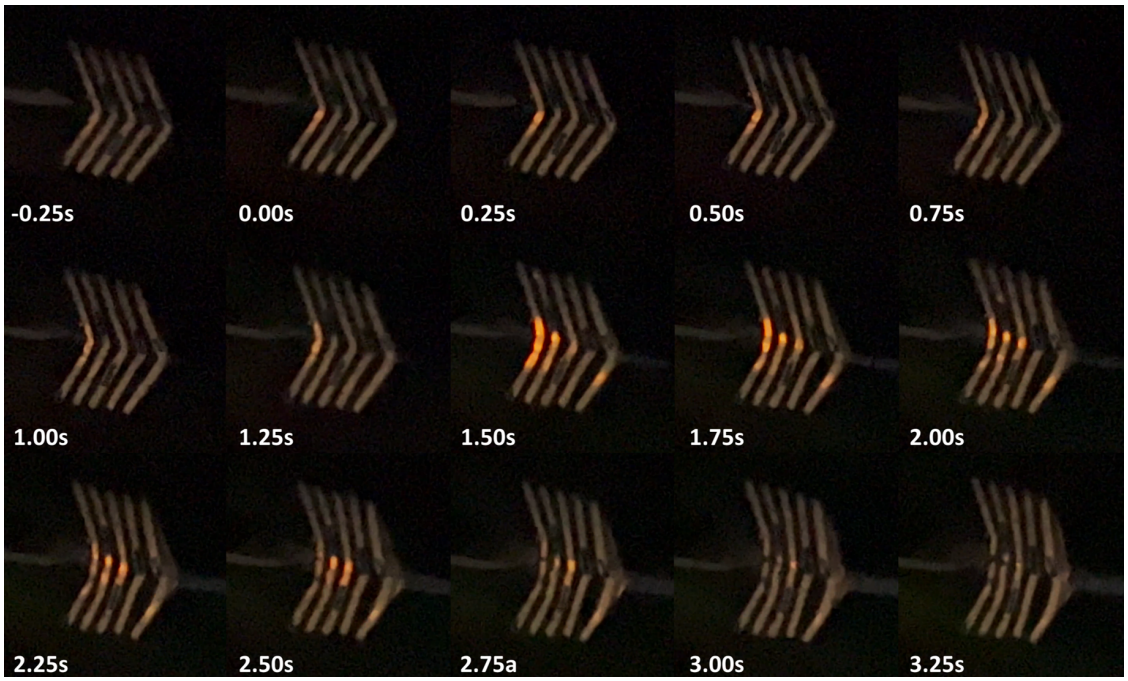

Figure 2. Time-lapse imagery of ML senor embedment with CT specimen undergoing crack initiation and propagation, with ML excitation and key junctures in the failure cycle.

As evident from Figure 2, the observed crack initiation and subsequent propagation exhibit distinct modes characterized by specific luminescent patterns present throughout the sample. The following outlines these modes to describe the depicted timelapse: 1) Undeformed State: Initially, prior to crack initiation there is an absence of observable luminescence. 2) Crack Initiation Excitation: As the mechanical load intensifies, localized stress concentrations become more prominent and triggers the generation of faint flashes of light at the crack tip. 3) Crack Propagation to 1st Notch: As the crack propagates, the luminescent activity becomes more pronounced, and the emitted light intensifies to reflect the increased energy release associated with crack advancement. 4) Subsequent Crack Propagation: The crack continues to propagate, unabated, through the material, reaching the 2nd to 5th sensor inclusions. This progression is visually evident as the crack front appears as an intensely illuminated region. 5) Final Notch Deformation: As the crack advances further, it reaches the final notch, resulting in notable deformation. The luminescent patterns exhibited by the material are fainter, as there are fewer sensors remaining in line with the crack. 6) Last Newly Created Face: At this stage, the crack has traversed the entire sample, resulting in the creation of a last newly formed face, representing the final state of the crack propagation process.

MECHANO-VISUALIZATION

The mechanical response of the ML-embedded samples under tensile loading was investigated, and ultimate tensile strength (UTS) and fracture energy (Gf) were measured for each sample type. Contextualizing the coupled relationship between the mechanical

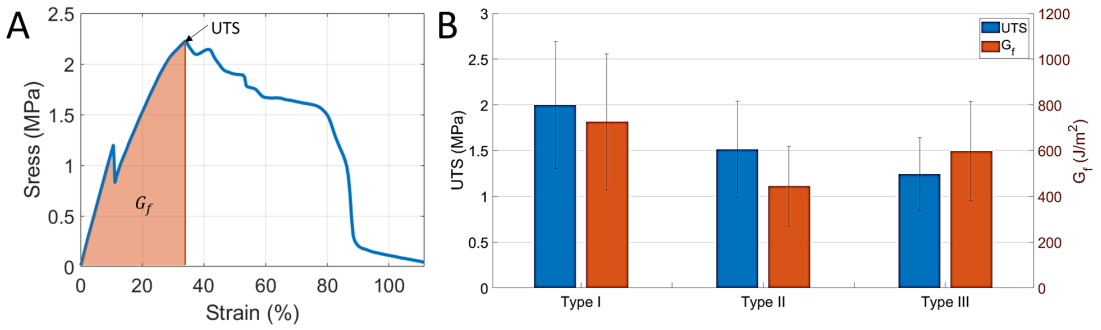

Figure 3. Typical CT specimen stress-strain graph showing UTS and Gf. (a) Comparative bar chart of UTS and Gf for three sample types (b).

strength and the luminescent response provides valuable insights into the underlying mechanisms governing ML in the context of tensile loading. The average UTS and Gf values for each sample type are summarized in Figure 3.

The observed trends in UTS and Gf provide insights into the structural integrity and mechanical robustness of the investigated materials. Sample Type 1, with the highest UTS and fracture energy, demonstrates superior mechanical properties, suggesting enhanced tensile strength and energy dissipation capability. In contrast, Sample Type 3 exhibits the lowest UTS but displays relatively higher fracture energy, indicating a potential trade-off between tensile strength and energy absorption from the different geometry of the embedded sensors. In the context of ML, a higher UTS suggests that the material can withstand higher levels of tensile stress before fracturing, suggesting corresponding light emittance may be more pronounced or intense in materials with higher UTS values due to the greater energy release during fracture processes. Conversely, a higher Gf value suggests that the material has a greater capacity to absorb and release energy during deformation and fracture processes, and as a result, may exhibit more prolonged ML responses.

ALGORITHMIC MATERIAL PLACEMENT

The algorithmic material placement approach presented in this section offers a structured pathway for determining potential locations to embed ML material within the compact tension sample. This process flow takes into consideration the local stress states induced by simulated loading conditions, aiming to strategically position the ML material for an optimal ML response. The resulting placement scheme is then utilized to generate a voxel representation of the sample's structure, which can be exported as an STL file for subsequent additive manufacturing processes. Iterative mechanical testing and inline visualization provide the necessary ML activation score to guide the placement of subsequently printed cavities for sensor embedment.

Figure 4A showcases the high-speed capture of ML during the loading of the sample. The captured ML signal is the primary response in which to correlate the temporal and spatial distribution of light emission, providing a direct visualization of the material's response to applied mechanical loads. Figure 4B presents an illustration depicting the

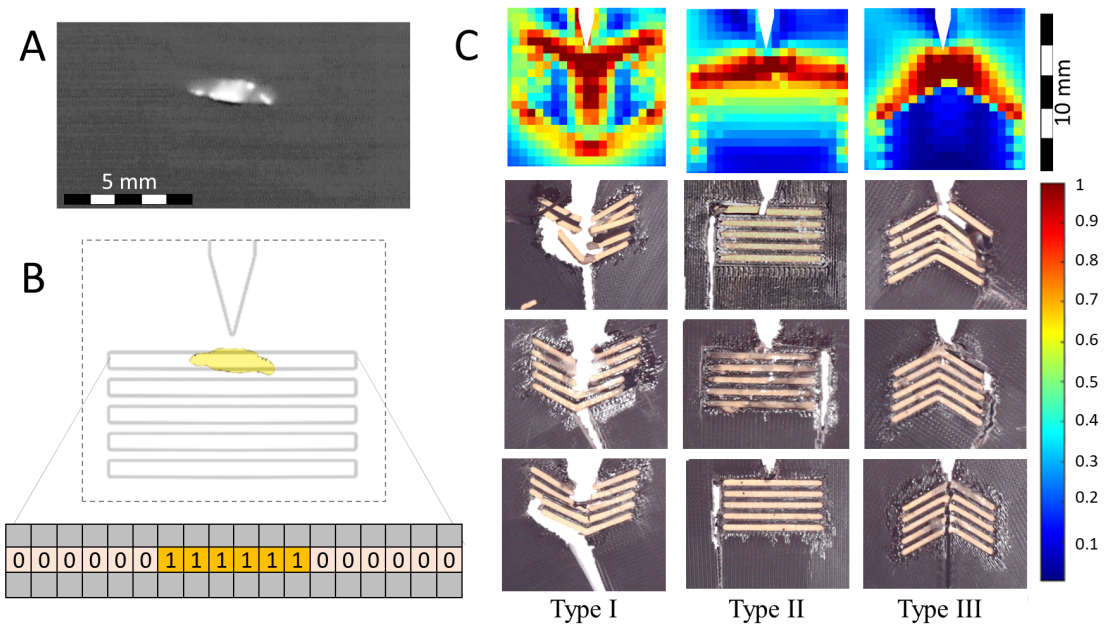

Figure 4. High-speed capture of ML during sample loading, providing a direct visualization of the material's response to mechanical loads (a) Illustration showing sensor allocation and its role in capturing the ML response during material deformation (b). Comparison of FEA results and fracture images, highlighting the correlation between crack growth and high local stress (c).

location and scale of 4A, while also presenting a graphical array to visualize the programmatic sensor allocation of our proposed method, where sensor light emittance is recorded in a binary state, effectively storing the locations of the sensors utilized during loading, highlights the strategic allocation of sensors and their role in capturing the ML response during material deformation. Figure 4C compares the finite element analysis (FEA) of each sample type with corresponding fracture images to demonstrate the correlation between crack growth and high local stress. It becomes apparent that crack growth corresponds significantly with areas of high local stress, suggesting crack propagation can, to a certain extent, be predicted based on the analysis of stress distribution to better inform sensor placement strategies.

Figure 5 presents a flowchart illustrating the eight steps of the algorithmic material placement approach. These steps involve 1) Stress Analysis – A comprehensive stress analysis to analyze the local stress states induced by simulated loading conditions. 2) ML Material Location Determination – favorable locations for embedding ML material within the sample are tabulated in relation to areas of high-stress concentration. 3) Voxel Representation Generation - A voxel representation of the sample's structure is generated, incorporating the determined ML material placement scheme. 4) STL File Export - The voxel representation is exported as an STL file for additive manufacturing processes. 5) Iterative Mechanical Testing and Visualization - The sample undergoes iterative mechanical testing while monitoring and capturing the ML response. 6) ML Activation Score Calculation - A quantitative metric indicating the effectiveness of the ML material placement scheme, aiding in decision-making for subsequent steps. 7)

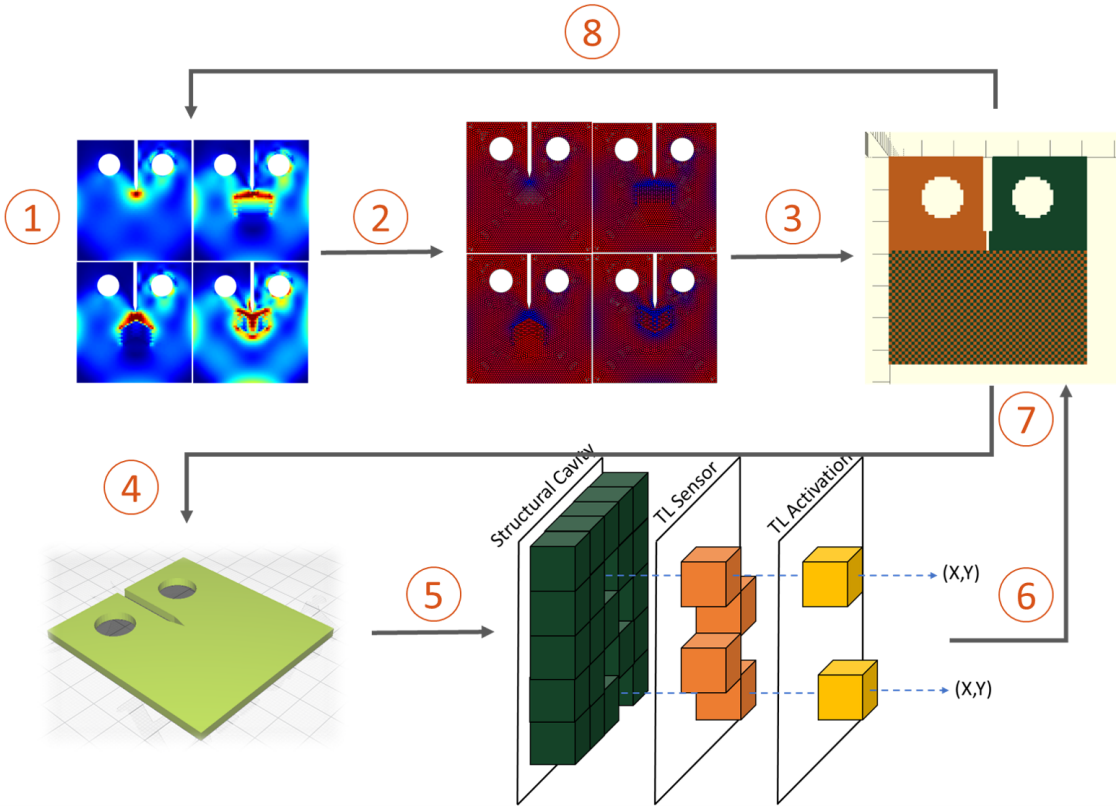

Figure 5. Flowchart illustrating the eight steps of the algorithmic material placement approach.

Guiding Cavity Placement - The locations and distribution of printed cavities for sensor embedment are determined within the sample. 8) Iterative Refinement - The material placement is refined and optimized through an iterative loop. By returning to Step 1, continuous improvement of the material placement scheme is ensured.

As a future prospect, this program architecture holds great potential for enhancement through the integration of machine learning techniques. By introducing a means in which to efficiently learn from previous sample geometries, an improved method to accurately allocates ML sensors in the unconstrained material placement process of AM. A future generalization of this method can contribute to streamlining decision-making capabilities by optimizing ML material placement, considering various factors such as material properties, loading conditions, and desired performance objectives throughout many different structures. This iterative improvement process, combined with the power of machine learning, can revolutionize the design and fabrication of ML-embedded structures, particularly for applications in structural health monitoring.

CONCLUSION

In conclusion, the visualization of ML and its integration into structural health monitoring present exciting opportunities for advancing the understanding and performance evaluation of next-generation materials. The use of high-speed video allows for real-

time observation of light emission during material deformation, providing valuable insights into the underlying mechanisms of ML. The correlation between ultimate tensile strength (UTS), fracture energy (Gf), and the intensity of ML further demonstrates the potential of this phenomenon as an evaluation tool in simulation. Additionally, the algorithmic material placement approach presented in this study offers a structured pathway for strategically embedding ML material within the sample, considering local stress states induced by simulated loading conditions. The proposed program architecture, coupled with machine learning, holds promise for iterative improvement and streamlining of ML-embedded structures for customized structural health monitoring. With continued research and development in this field, ML has the potential to revolutionize material characterization and facilitate the design of more robust and resilient structures for a wide range of applications.

ACKNOWLEDGMENT

The authors would like to thank the High Performance Materials Institute (HPMI) for the use of laboratory space and the supportive environment of the FAMU-FSU College of Engineering.

REFERENCES

1. Olawale, D. O., R. S. Fontenot, M. A. S. Shohag, and O. O. I. Okoli. 2016. "Introduction to Triboluminescence," in D. O. Olawale, O. O. I. Okoli, R. S. Fontenot, and W. A. Hollerman, eds., *Triboluminescence: Theory, Synthesis, and Application*, Springer International Publishing, Cham, ISBN 978-3-319-38842-7, pp. 1–16, doi:10.1007/978-3-319-38842-7_1.
2. Psulkowski, S., M. Pollard, S. Jackson, P. Tran, and T. Dickens. 2019. "Intelligent Processes and Operational Monitoring of Composite Systems," *Structural Health Monitoring 2019*, 0(0), doi:10.12783/shm2019/32208.
3. Shohag, M. A., Y.-S. Dessureault, K. Joshi, T. Ndebele, D. Olawale, T. Dickens, and O. Okoli. 2018. "Enhanced fabrication process for in situ triboluminescent optical fiber sensor for multifunctional composites," *Measurement*, 121:240–248, ISSN 0263-2241, doi:10.1016/j.measurement.2018.02.051.
4. Leelachao, S., S. Muraishi, T. Sannomiya, J. Shi, and Y. Nakamura. 2016. "Correlation of triboluminescence and contact stresses in ZnS:Mn/polymeric matrix composite," *Journal of Luminescence*, 170:24–29, ISSN 0022-2313, doi:10.1016/j.jlumin.2015.10.009.